

Magnetic Double Structure for $S = 1, 1/2$ Mixed-Spin Systems

Yoshihiro Takushima, Akihisa Koga, and Norio Kawakami
Department of Applied Physics, Osaka University, Suita, Osaka 565-0871, Japan
(November 5, 2018)

We investigate the zero-temperature and the finite-temperature properties of the two-dimensional antiferromagnetic quantum spin system composed of the $s = 1/2$ and $s = 1$ spins. The spin excitation spectrum as well as the thermodynamic quantities are computed by means of the Schwinger-boson mean-field theory. We discuss how the magnetic double structure with the gapful and the gapless excitations is generated, and apply the results systematically to the Haldane gap system in a staggered magnetic field and also to the weakly coupled ferrimagnetic mixed-spin chains. It is confirmed that the results obtained are consistent with the experiments for the quasi-one-dimensional Haldane compounds $R_2\text{BaNiO}_5$.

I. INTRODUCTION

The Haldane gap system¹ has been one of the most fascinating subjects in condensed matter physics, for which extensive experimental and theoretical investigations have been providing a variety of new interesting phenomena. One of the hot topics is the magnetic double structure in the quasi-one-dimensional (1D) Haldane systems observed for the rare-earth compounds $R_2\text{BaNiO}_5$.²⁻⁷ In the case with $R = \text{Y}^{3+}$, the system has a disordered ground state with the Haldane gap.⁸ If R is substituted by other magnetic ions such as Nd^{3+} and Pr^{3+} ,^{7,9} the $s = 1/2$ spins on the R^{3+} sublattice order magnetically at low temperatures, thus giving rise to the magnetic double structure composed of the Haldane gap excitation and the gapless excitation induced by the long-range order. This system has been theoretically treated as the Haldane chains with a *static* staggered field which are induced by the ordered $s = 1/2$ spins on the R^{3+} sublattice so far.^{10,11} In a recent paper,⁵ however, it has been pointed out that the dynamics of the $s = 1/2$ spins may be also important, stimulating us to treat the system by a mixed-spin model. Concerning the magnetic double structure, there is another interesting spin system of current interest, i.e. the quantum ferrimagnetic chain composed of two kinds of mixed spins.¹²⁻¹⁷ Several compounds have been already found, which indeed realize the mixed-spin system.^{12,13} This has been stimulating further intensive theoretical studies on this subject.¹⁴⁻¹⁷ In particular, it has been pointed out that such a ferrimagnetic chain has the double structure for the spin excitation spectrum, which controls the characteristic properties in the ferrimagnetic chain.¹⁶

The above two subjects, which have been studied experimentally in different contexts, should possess the common interesting physics, because both systems are

characterized by the mixture of two kinds of distinct spins. Motivated by these hot topics, we here study the properties of the antiferromagnetic mixed-spin system in detail, for which the $s = 1$ and $s = 1/2$ spin chains are stacked alternately. We exploit the two-dimensional (2D) system as the simplest model which possesses the magnetic long-range order at zero temperature. By computing the dispersion relation and the staggered magnetization by means of the Schwinger-boson mean-field theory,¹⁸ we clarify how our system generates the magnetic double structure, which naturally interpolates the above two interesting spin systems. We also show that the results obtained are consistent with the experimental findings for quasi-1D Haldane compounds $R_2\text{BaNiO}_5$.²⁻⁷

This paper is organized as follows. We introduce the model and then briefly summarize the Schwinger-boson techniques in Sec. II. We discuss the zero-temperature properties in Sec. III, and finally move to the thermodynamic properties in Sec. IV. A brief summary is given in Sec. V.

II. SCHWINGER-BOSON MEAN-FIELD THEORY

Let us consider a 2D mixed-spin model on the square lattice, which is described by the following Hamiltonian,

$$H = J_1 \sum_{i,j,\eta} \left[\mathbf{S}_{2i,2j}^{A_1} \cdot \mathbf{S}_{2i+\eta,2j}^{B_1} + \mathbf{S}_{2i+\eta,2j+1}^{B_2} \cdot \mathbf{S}_{2i,2j+1}^{A_2} \right] \\ + \sum_{i,j,\eta} \left[J_2 \mathbf{S}_{2i,2j}^{A_1} \cdot \mathbf{S}_{2i,2j+\eta}^{A_2} + J_3 \mathbf{S}_{2i+1,2j}^{B_1} \cdot \mathbf{S}_{2i+1,2j+\eta}^{B_2} \right], \quad (1)$$

where $\mathbf{S}_{i,j}^A$ ($\mathbf{S}_{i,j}^B$) is the spin operator at the (i,j) -th site in the (x,y) plane, and η implies the summation to be taken over nearest-neighbor sites. All the exchange couplings J_1 , J_2 and J_3 are assumed to be antiferromagnetic. We here focus on the mixed-spin system composed of $S^A = 1/2$ and $S^B = 1$ spins, since it is straightforward to generalize the results to the arbitrary-spin case. In Fig. 1, we have drawn the mixed-spin model schematically. The indices A_m and B_m label the sublattice in the unit cell. Note that this mixed-spin model is constructed in two ways depending on how we stack the independent spin chains by introducing three kinds of the coupling constants. By taking $J_3 \gg J_1, J_2$, we can study the characteristic properties of the $s = 1$ Haldane spin chains coupled with the $s = 1/2$ gapless spin chains, which may have the relevance to the Haldane gap system in a staggered field observed in the compounds $R_2\text{BaNiO}_5$.²⁻⁷ On the other hand, by setting the coupling constants

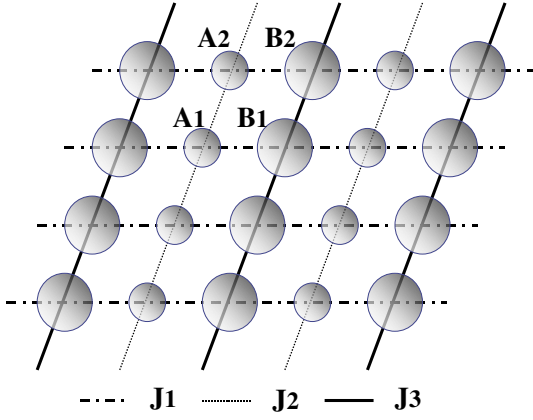


FIG. 1. 2D mixed-spin model on a square lattice. The small (large) circle represents $S^A = 1/2$ ($S^B = 1$) spin. The bold dashed, the thin dashed and the bold solid lines represent the coupling constants J_1 , J_2 and J_3 , respectively. A_1, A_2, B_1 and B_2 specify four spins in the unit cell.

$J_1 \gg J_2, J_3$, we can investigate how the independent ferromagnetic chains ($J_2 = J_3 = 0$), which have been studied extensively in recent years,^{12–17} are combined to form the 2D system. The advantage of our mixed-spin approach is that we can systematically describe these two interesting systems by continuously varying the parameters J_1 , J_2 and J_3 .

We employ the Schwinger-boson mean-field theory (SBMFT)¹⁸ to study the above mixed-spin model.¹⁹ This method was applied successfully to the 2D Heisenberg model with uniform spins,^{18,20} and then to the bilayer system,²¹ the double-exchange system,²² the ferrimagnetic chain,¹⁷ etc. It is known that the SBMFT can describe the magnetically ordered phase, which is characterized by the condensation of the Schwinger-bosons.²⁰ In the Schwinger-boson representation, the spin operators are expressed in terms of the boson creation and annihilation operators $\gamma_\alpha^\dagger, \gamma_\alpha$, with the Pauli matrix σ as $\mathbf{S} = \frac{1}{2}\gamma_\alpha^\dagger \sigma_{\alpha\beta} \gamma_\beta$ ($\alpha, \beta = \uparrow, \downarrow$). Since the unit cell in our model includes four sites, we necessarily introduce eight kinds of Bose operators $\gamma_\alpha = a_\alpha^{(1)}, a_\alpha^{(2)}, b_\alpha^{(1)}, b_\alpha^{(2)}$ which belong to the A_1, A_2, B_1, B_2 sublattices, respectively. By imposing the constraint $\gamma_{i\uparrow}^\dagger \gamma_{i\uparrow} + \gamma_{i\downarrow}^\dagger \gamma_{i\downarrow} = 2S^A$ or $2S^B$ on each site, we can correctly map the original spin system to the boson system. Introducing the Lagrange multipliers λ_{ij}^A and λ_{ij}^B , the Hamiltonian with the constraints is recast to

$$\begin{aligned}
H = & -2 \sum_{i,j,\eta} \left[J_1 \left(A_{ij\eta}^\dagger A_{ij\eta} + B_{ij\eta}^\dagger B_{ij\eta} \right) \right. \\
& + J_2 C_{ij\eta}^\dagger C_{ij\eta} + J_3 D_{ij\eta}^\dagger D_{ij\eta} \left. \right] \\
& + \sum_{n=1}^2 \left[\sum_{(ij) \in A_n} \lambda_{ij}^A \left(\sum_{\sigma} a_{ij\sigma}^{(n)\dagger} a_{ij\sigma}^{(n)} - 2S^A \right) \right.
\end{aligned}$$

$$\begin{aligned}
& + \sum_{(ij) \in B_n} \lambda_{ij}^B \left(\sum_{\sigma} b_{ij\sigma}^{(n)\dagger} b_{ij\sigma}^{(n)} - 2S^B \right) \left. \right] \\
& + \sum_{i,j,\eta} \left[J_1 (S^{A_1} S^{B_1} + S^{A_2} S^{B_2}) \right. \\
& + J_2 S^{A_1} S^{A_2} + J_3 S^{B_1} S^{B_2} \left. \right], \quad (2)
\end{aligned}$$

where four bond operators are introduced as

$$A_{ij\eta} = a_{2i,2j\uparrow}^{(1)} b_{2i+\eta,2j\downarrow}^{(1)} - a_{2i,2j\downarrow}^{(1)} b_{2i+\eta,2j\uparrow}^{(1)}, \quad (3)$$

$$B_{ij\eta} = a_{2i,2j+1\uparrow}^{(2)} b_{2i+\eta,2j+1\downarrow}^{(2)} - a_{2i,2j+1\downarrow}^{(2)} b_{2i+\eta,2j+1\uparrow}^{(2)}, \quad (4)$$

$$C_{ij\eta} = a_{2i,2j\uparrow}^{(1)} a_{2i,2j+\eta\downarrow}^{(2)} - a_{2i,2j\downarrow}^{(1)} a_{2i,2j+\eta\uparrow}^{(2)}, \quad (5)$$

$$D_{ij\eta} = b_{2i+1,2j\uparrow}^{(1)} b_{2i+1,2j+\eta\downarrow}^{(2)} - b_{2i+1,2j\downarrow}^{(1)} b_{2i+1,2j+\eta\uparrow}^{(2)}. \quad (6)$$

We perform a Hartree-Fock decomposition of eq. (2) by taking the thermal average $\langle A_{ij\eta} \rangle = A$, $\langle \lambda_{ij}^A \rangle = \lambda_A$, etc., which means that these values are assumed to be uniform and static.

By diagonalizing the mean-field Hamiltonian via the Bogoliubov transformation, we have

$$H_{\text{MF}} = \sum_{\mathbf{k}\sigma} \sum_{n=1}^2 \left[E_{\mathbf{k}}^{(1)} \alpha_{\mathbf{k}\sigma}^{(n)\dagger} \alpha_{\mathbf{k}\sigma}^{(n)} + E_{\mathbf{k}}^{(2)} \beta_{\mathbf{k}\sigma}^{(n)\dagger} \beta_{\mathbf{k}\sigma}^{(n)} \right], \quad (7)$$

where α and β are the Bose operators for normal modes. The corresponding energy spectrums read

$$E_{\mathbf{k}}^{(1)} = \sqrt{\frac{E_0 - \sqrt{E_1}}{2}}, \quad E_{\mathbf{k}}^{(2)} = \sqrt{\frac{E_0 + \sqrt{E_1}}{2}}, \quad (8)$$

where E_0 and E_1 are given by

$$\begin{aligned}
E_0 = & \lambda_A^2 + \lambda_B^2 - 2d_{\mathbf{k}}^2 - e_{\mathbf{k}}^2 - f_{\mathbf{k}}^2, \\
E_1 = & (\lambda_A^2 - \lambda_B^2 - e_{\mathbf{k}}^2 + f_{\mathbf{k}}^2)^2 \\
& - 4d_{\mathbf{k}}^2 \left((\lambda_A - \lambda_B)^2 - (e_{\mathbf{k}} + f_{\mathbf{k}})^2 \right), \quad (9)
\end{aligned}$$

with

$$\begin{aligned}
d_{\mathbf{k}} = & 2AJ_1 \cos k_x, \quad e_{\mathbf{k}} = 2CJ_2 \cos k_y, \\
f_{\mathbf{k}} = & 2DJ_3 \cos k_y.
\end{aligned}$$

By minimizing the free energy thus obtained at finite temperatures, we end up with the self-consistent equations for $A = B, C, D, \lambda_A, \lambda_B$,

$$1 + 2S^A = \sum_n \int \frac{d\mathbf{k}}{\pi^2} \coth \kappa E_{\mathbf{k}}^{(n)} \frac{\partial E_{\mathbf{k}}^{(n)}}{\partial \lambda_A}, \quad (10)$$

$$1 + 2S^B = \sum_n \int \frac{d\mathbf{k}}{\pi^2} \coth \kappa E_{\mathbf{k}}^{(n)} \frac{\partial E_{\mathbf{k}}^{(n)}}{\partial \lambda_B}, \quad (11)$$

$$-8J_1 A = \sum_n \int \frac{d\mathbf{k}}{\pi^2} \coth \kappa E_{\mathbf{k}}^{(n)} \frac{\partial E_{\mathbf{k}}^{(n)}}{\partial A}, \quad (12)$$

$$-4J_2C = \sum_n \int \frac{d\mathbf{k}}{\pi^2} \coth \kappa E_{\mathbf{k}}^{(n)} \frac{\partial E_{\mathbf{k}}^{(n)}}{\partial C}, \quad (13)$$

$$-4J_3D = \sum_n \int \frac{d\mathbf{k}}{\pi^2} \coth \kappa E_{\mathbf{k}}^{(n)} \frac{\partial E_{\mathbf{k}}^{(n)}}{\partial D}, \quad (14)$$

with $\kappa = 1/(2k_B T)$, where we have assumed that the bond operators which link the $s = 1$ and $s = 1/2$ spins take the same mean value, $A = B$. This completes our formulation based on the SBMFT. In the following sections, we solve these self-consistent equations to estimate the excitation spectrum and the thermodynamic quantities. Since it is not easy to analytically perform the Bogoliubov transformation, we numerically diagonalize the mean-field Hamiltonian to compute the energy dispersions $E_{\mathbf{k}}^{(1)}$ and $E_{\mathbf{k}}^{(2)}$.

III. PROPERTIES AT ZERO TEMPERATURE

In order to treat the ground state properties, it should be taken into account that the Bogoliubov particles of the α branch in eq.(7) may condense at absolute zero, because the excitation energy $E_{\mathbf{k}}^{(1)}$ has its minimal value $E_{\mathbf{k}}^{(1)} = 0$ at $\mathbf{k} = \mathbf{0}$ while the β branch has a finite gap even at $T = 0$. Sarker *et al.*²⁰ showed that the long-range order is described by the condensation of the Schwinger-bosons for the ferromagnetic and antiferromagnetic Heisenberg models. This is also the case for our 2D mixed-spin model on a square lattice.

Suppose that the bosons condense at the states of $\alpha_{\uparrow}^{(1)}|_{\mathbf{k}=\mathbf{0}}$ and $\alpha_{\downarrow}^{(2)}|_{\mathbf{k}=\mathbf{0}}$, by fictitiously applying an infinitesimal external staggered field to the A and B lattices. The self-consistent equations at $T = 0$, which include the Bose condensation, now read,

$$\Gamma = \frac{2}{N^2} \coth \kappa E_{\mathbf{k}=\mathbf{0}}^{(1)} \Big|_{\kappa \rightarrow \infty} = \frac{\left[1 + 2S^A - \sum_n \int \frac{d\mathbf{k}}{\pi^2} \frac{\partial E_{\mathbf{k}}^{(n)}}{\partial \lambda_A} \right]}{\partial E_{\mathbf{k}=\mathbf{0}}^{(1)} / \partial \lambda_A}, \quad (15)$$

$$1 + 2S^B = \Gamma \frac{\partial E_{\mathbf{k}}^{(1)}}{\partial \lambda_B} \Big|_{\mathbf{k}=\mathbf{0}} + \sum_n \int \frac{d\mathbf{k}}{\pi^2} \frac{\partial E_{\mathbf{k}}^{(n)}}{\partial \lambda_B}, \quad (16)$$

$$-4A = \Gamma \frac{\partial E_{\mathbf{k}}^{(1)}}{\partial d_{\mathbf{k}}} \Big|_{\mathbf{k}=\mathbf{0}} + \sum_n \int \frac{d\mathbf{k}}{\pi^2} \cos k_x \frac{\partial E_{\mathbf{k}}^{(n)}}{\partial d_{\mathbf{k}}}, \quad (17)$$

$$-2C = \Gamma \frac{\partial E_{\mathbf{k}}^{(1)}}{\partial e_{\mathbf{k}}} \Big|_{\mathbf{k}=\mathbf{0}} + \sum_n \int \frac{d\mathbf{k}}{\pi^2} \cos k_y \frac{\partial E_{\mathbf{k}}^{(n)}}{\partial e_{\mathbf{k}}}, \quad (18)$$

$$-2D = \Gamma \frac{\partial E_{\mathbf{k}}^{(1)}}{\partial f_{\mathbf{k}}} \Big|_{\mathbf{k}=\mathbf{0}} + \sum_n \int \frac{d\mathbf{k}}{\pi^2} \cos k_y \frac{\partial E_{\mathbf{k}}^{(n)}}{\partial f_{\mathbf{k}}}. \quad (19)$$

We shall solve these equations numerically for given coupling constants J_1, J_2 and J_3 .

A. Dispersion relation

We start our discussions with the case that may be regarded as the Haldane gap system in a staggered field. When $J_1 = 0$, the 2D system is completely decoupled into the $s = 1$ massive Haldane chains and the $s = 1/2$ massless spin chains. When we introduce the interchain couplings among them, the ground state has the long-range order mainly due to the $s = 1/2$ spins. The important point is that even though we have the long-range order, the Haldane-type gapful excitation still exists. Therefore, as far as the case with small J_1 and J_2 is concerned, the system is regarded as the one often called the Haldane gap system in a staggered field.²⁻⁷ In Fig. 2, we show the dispersion relation calculated for $J_1 = J_2 = 1/2$ and $J_3 = 1$. As seen in this figure, the lower branch

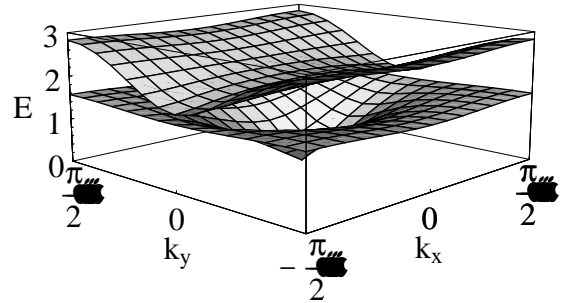


FIG. 2. The excitation spectrum for the mixed-spin model which may be regarded as the *Haldane gap in a staggered field* ($J_1 = J_2 = 1/2, J_3 = 1$). Note that the Brillouin zone is reduced to a quarter of that for the uniform spin case, since the unit cell now includes the four sites.

is gapless with linear dispersion relation, reflecting the antiferromagnetic long-range order, whereas the upper optical mode is mainly composed of the Haldane-type excitation. It is observed that the dispersion in the k_x -direction is indeed weak for the optical mode, since the interchain coupling is much smaller than the energy gap for the optical mode, which confirms that the system in Fig. 2 may be regarded as the Haldane gap system in a staggered field. Although we have also performed the calculation for the cases with smaller J_1 and J_2 , the obtained dispersion of the optical branch becomes almost flat in the k_x -direction, so that we have not shown them here. Concerning this limit of small J_1 , we here make a brief comment on the validity of the SBMFT. When J_1 takes too small value, for which the system is almost decoupled into independent $s = 1$ and $s = 1/2$ chains, the SBMFT may lead to a pathological result: although the Haldane gap for the $s = 1$ chain is well described by the SBMFT, it is not the case for the gapless $s = 1/2$ chains, for which we are left with a gapful phase. Actually, if the value of J_1 ($= J_2$) becomes smaller than $J_1/J_3 \sim 10^{-2}$,

we encounter a problem that the present self-consistent calculation does not converge, implying that our assumption for the antiferromagnetic ordered state does not hold anymore. Nevertheless, we find that the correct behavior with the antiferromagnetic ground state is still obtained except for this small parameter region.

By increasing the coupling parameters J_2, J_3 continuously, we naturally enter in the 2D ordered mixed-spin system. Note that although during this process the magnetic double structure is kept unchanged in its typical feature, the nature of the optical mode is gradually changed from the Haldane-gap excitation: i.e. the gapful excitation may be equally contributed from both the $s = 1$ and $s = 1/2$ spin sectors. As a reference, we show the dispersion relation for the mixed-spin model with the isotropic bonds $J_1 = J_2 = J_3 = 1$ in Fig. 3. If we further decrease

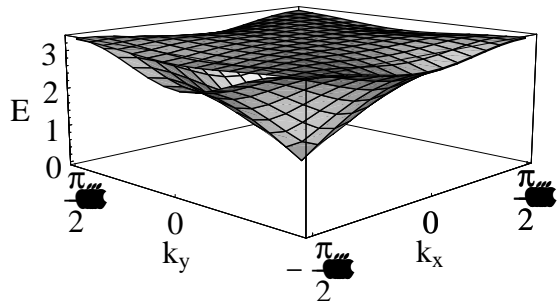


FIG. 3. The excitation spectrum for the 2D mixed-spin model ($J_1 = J_2 = J_3 = 1$).

the couplings J_2 and J_3 , the system gradually approaches the quasi-1D ferrimagnetic chains with the periodic arrangement of spins $1/2 \circ 1 \circ 1/2 \circ 1$. The dispersion relation obtained in the corresponding parameter region is shown in Fig. 4. Now the optical mode with a weak disper-

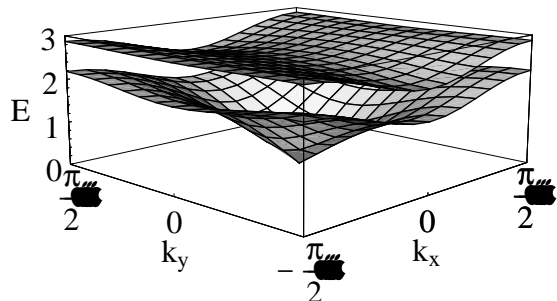


FIG. 4. The excitation spectrum for the *coupled ferrimagnetic chains* ($J_1 = 1, J_2 = J_3 = 1/2$).

sion in the k_y -direction is essentially the same as that found for the ferrimagnetic chain.¹⁶ In order to clearly observe how the gapless dispersion changes its character in the ferrimagnetic-chain limit, we have shown the low-energy dispersion relation at $k_y=0$ in Fig. 5. It is seen that with the decrease of the coupling constants J_2 and J_3 , the k_x -linear dependence is gradually changed to the k_x^2 dependence characteristic of the ferrimagnetic chain except for the small k_x region where the 2D an-

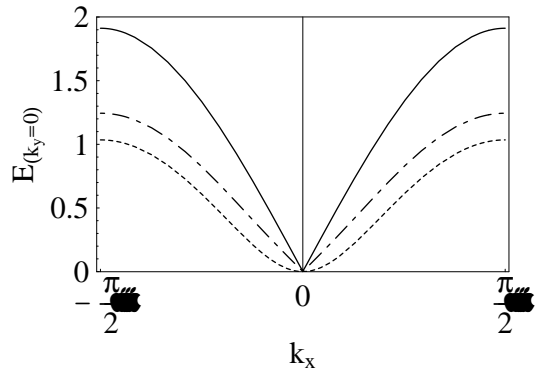


FIG. 5. The gapless dispersion for the *coupled ferrimagnetic chains* at $k_y=0$. The solid, the dash-dotted and the dashed lines correspond to the cases of $J_2 = J_3 = 0.5, 0.1$ and 0 ($J_1 = 1$).

tiferromagnetic order still gives rise to the k_x -linear dependence. At $J_2 = J_3 = 0$, the system is reduced to the isolated ferrimagnetic chains, for which the 2D character completely disappears, and thus the gapless dispersion simply follows the k_x^2 dependence. We note that the ferrimagnetic chains have been experimentally realized in the compounds such as $\text{NiCu}(\text{C}_2\text{O}_4)_2 \cdot 4\text{H}_2\text{O}$ and $\text{MnCu}(\text{pba})(\text{H}_2\text{O})_3 \cdot 2\text{H}_2\text{O}$,¹³ and have been studied theoretically by many groups.^{14–16} Among others, it has been reported¹⁶ that this system exhibits the dual properties consistent with our results: the physical quantities are controlled by the $s = 1$ antiferromagnetic spin chain at high temperatures and by the effective $s = 1/2$ ferromagnetic spin chain at low temperatures.

The above analysis of the excitation spectrum implies that the quasi-1D Haldane gap system in a staggered field^{2–7} and the quasi-1D weakly coupled ferrimagnetic chains,^{12,13} which have been studied in different contexts experimentally, share common interesting physics inherent in the mixed-spin systems. In particular, it is highly desirable to experimentally observe the magnetic double structure in the excitation spectrum for the ferrimagnetic-chain compounds.

B. Haldane gap in a staggered field

Let us discuss the case of the Haldane gap system in a staggered field in more detail. We here observe how the effective staggered field induced by the $s = 1/2$ spin chains affects the properties of the Haldane gap, by changing the coupling constants J_1 and J_2 . For small values of J_1 and J_2 , we define the effective staggered field on the $s = 1$ Haldane chain by $H_{\text{ST}}^{\text{eff}} = J_1 \langle S_z^A \rangle$, where $\langle S_z^A \rangle$ is the spontaneous staggered magnetization of the $s = 1/2$ spin chain. We numerically estimate the effective staggered field, and show the obtained results in Fig. 6. It is seen that the effective staggered field increases monotonously with the increase of J_1 and J_2 , as should be expected. In a similar way, we also compute

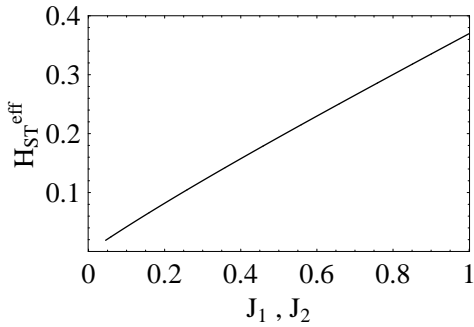


FIG. 6. The effective staggered field $H_{\text{ST}}^{\text{eff}}$ as a function of the coupling constant J_1 ($=J_2$) where we set $J_3 = 1$.

the staggered magnetization $\langle S_z^B \rangle$ of the $s = 1$ spin chains, and as well as the Haldane gap which is defined as the minimum of the excitation energy in the optical branch $\Delta = E_{\mathbf{k}=(\frac{\pi}{2},0)}^{(2)}$. These quantities are shown in

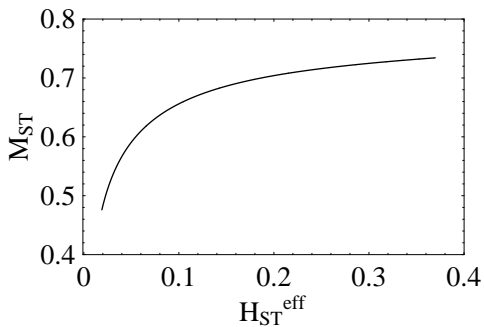


FIG. 7. Plots of the staggered magnetization M_{ST} as a function of the effective staggered magnetic field.

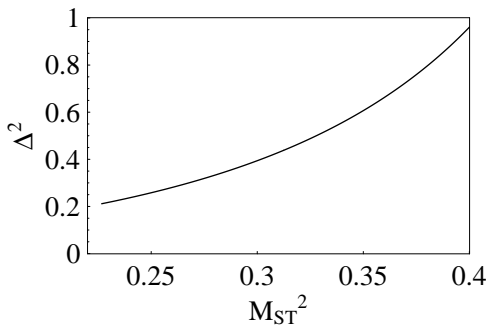


FIG. 8. Plots of the square of the Haldane gap Δ as a function of the square of the staggered magnetization M_{ST} .

Figs. 7 and 8. Following the way used for the experimental analysis,^{2,4} we have plotted the staggered magnetization (the square of the Haldane gap) as a function of the effective staggered field (the square of the staggered magnetization). It is seen that as the staggered field is increased, the staggered magnetization as well as the Haldane gap Δ are increased, being consistent with the result pointed out for the Haldane chain system with a *static* magnetic field.^{10,11}

Since we are dealing with the 2D model at zero temperature, our results may not be directly applied to the experiments. Nevertheless, we can confirm whether the present results are consistent with the experiments for the rare-earth compounds $R_2\text{BaNiO}_5$ ²⁻⁷ with $R = \text{Nd}^{3+}$ or Pr^{3+} .^{7,9} Experimentally, as the temperature is decreased, the system shows the phase transition to the magnetically ordered phase. When the temperature is further decreased, the staggered moment for the $s = 1/2$ sector develops, and thereby gives rise to the increase of the staggered field, which indeed enhances the magnitude of the Haldane gap.^{10,11} Also, the staggered moment on the Haldane chains increases, as should be expected. These characteristic features are consistent with our results, and in particular, the qualitative behaviors for the staggered magnetization and the Haldane gap shown in Figs. 7 and 8 agree fairly well with experimental findings.^{2,4}

C. Coupled ferrimagnetic chains

Before closing this section, we briefly discuss the case close to the ferrimagnetic chain, which is realized by taking the limit of $J_1 \gg J_2, J_3$. Even in this one-dimensional limit, the system still exhibits the antiferromagnetic order as far as J_2 and J_3 take finite values. As mentioned above, at $J_2 = J_3 = 0$, the system shows the ferrimagnetic order, and hence the dispersion relation for the acoustic mode is changed to the quadratic one.¹⁵⁻¹⁷ In this way, the crossover-like behavior is seen in the gapless mode, whereas much simpler behavior is observed in the gapful mode. In Fig. 9, we display the spin gap Δ for the optical branch in the ferrimagnetic-chain limit. With decreasing J_2 and J_3 , the spin gap monotonically decreases, and reaches the value of $\Delta=1.778$ at $J_2 = J_3 = 0$, which is very close to that of the quantum Monte Carlo method, $\Delta=1.767$,¹⁵ as already demonstrated by Wu *et al.*¹⁷ In this way, in the ferrimagnetic-chain limit, the SBMFT may provide the reliable estimates of the physical quantities even at quantitative level. As discussed by Yamamoto and Fukui,¹⁶ this optical mode is mainly composed of excitations in the effective $s = 1$ antiferromagnetic spin chain, whereas the acoustic mode is given by excitations in the effective $s = 1/2$ ferromagnetic chain.

IV. THERMODYNAMIC PROPERTIES AT FINITE TEMPERATURES

We now move to the thermodynamic properties at finite temperatures. The self-consistent equations (10)-(14) are solved numerically at finite temperatures to obtain the thermodynamic quantities. We here briefly summarize the results obtained. In the previous section, it has been shown that even for the set of the parameters $J_1 = J_2 = 1/2, J_3 = 1$ ($J_1 = 1, J_2 = J_3 = 1/2$), the

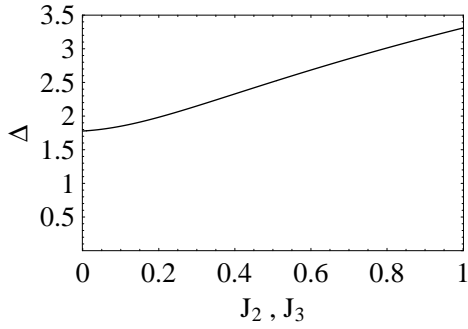


FIG. 9. Plots of the spin gap for the optical branch in the limit of the coupled ferrimagnetic chains ($J_2 = J_3$).

system may be approximately described by the Haldane gap system in a staggered field (coupled ferrimagnetic chains), so that we shall show the results for these parameters below. We start with the effective spin gaps

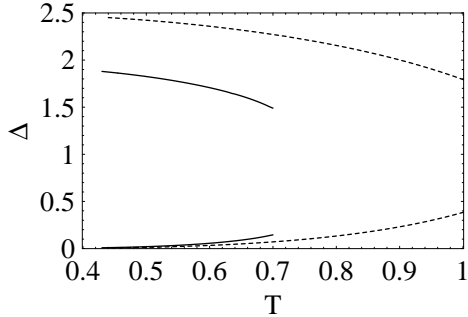


FIG. 10. The spin gaps for the optical and acoustic branches as a function of the temperature T : the solid lines correspond to the case for $J_1 = J_2 = 1/2, J_3 = 1$ while the dashed lines for $J_1 = 1, J_2 = J_3 = 1/2$. Note that at higher temperatures our SBMF approach breaks down, so that we have plotted the data available for each choice of parameters.

calculated at finite temperatures, which are shown as a function of the temperature in Fig. 10. It is seen that both of the two cases exhibit similar temperature dependence in the spin gap. For each case, there are two distinct spin gaps, corresponding respectively to the optical mode and the acoustic mode, reflecting the double structure for the excitation spectrum. Note that both of two modes should be massive at finite temperatures. It may be physically sensible to regard these spin gaps as the inverse of the correlation lengths. As should be expected, the spin gap for the optical mode increases up to the zero-temperature value with the decrease of the temperature. On the other hand, the spin gap for the acoustic mode decreases, leading to the divergent correlation length which characterizes the magnetically ordered state at $T = 0$.

The uniform and staggered spin susceptibilities, χ_{uni} and χ_{stag} , are calculated by using the standard linear-response formulae,

$$\chi_{\text{uni}} = \sum_{i,j=1,2} [\langle \langle S_z^{A_i} S_z^{A_j} \rangle \rangle_{\mathbf{q},\omega} + \langle \langle S_z^{B_i} S_z^{B_j} \rangle \rangle_{\mathbf{q},\omega} + 2\langle \langle S_z^{A_i} S_z^{B_j} \rangle \rangle_{\mathbf{q},\omega}] |_{\mathbf{q},\omega \rightarrow 0}, \quad (20)$$

$$\chi_{\text{stag}} = \sum_{i,j=1,2} [(-1)^{i+j} (\langle \langle S_z^{A_i} S_z^{A_j} \rangle \rangle_{\mathbf{q},\omega} + \langle \langle S_z^{B_i} S_z^{B_j} \rangle \rangle_{\mathbf{q},\omega}) + 2(-1)^{i+j+1} \langle \langle S_z^{A_i} S_z^{B_j} \rangle \rangle_{\mathbf{q},\omega}] |_{\mathbf{q},\omega \rightarrow 0}, \quad (21)$$

where $\langle \langle S_z^{A_i} S_z^{A_j} \rangle \rangle_{\mathbf{q},\omega}$, etc., are the retarded spin correlation functions. In Fig. 11, we plot the effective Curie

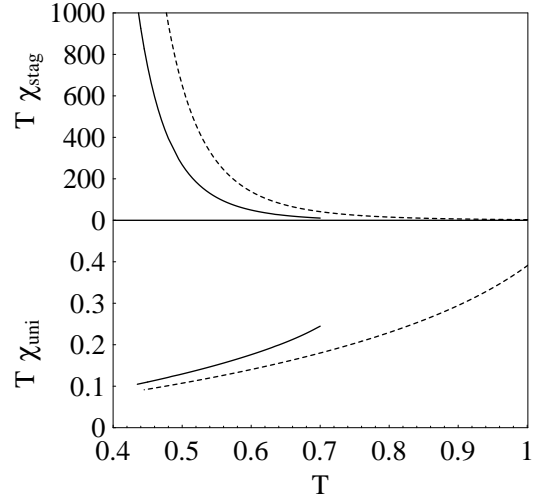


FIG. 11. Plots of $T\chi_{\text{stag}}$ for the staggered susceptibility and $T\chi_{\text{uni}}$ for the uniform susceptibility as a function of the temperature T : the solid lines for $J_1 = J_2 = 1/2, J_3 = 1$ and the dashed lines for $J_1 = 1, J_2 = J_3 = 1/2$

constants $T\chi_{\text{uni}}$ and $T\chi_{\text{stag}}$ as a function of T . It is seen that the effective Curie constant for the uniform sector is gradually decreased as the temperature is decreased, while that for the staggered sector diverges, implying that the antiferromagnetic correlation is enhanced at low temperatures.

As seen from the above results, the thermodynamic properties at finite temperatures show quite similar behavior both for the Haldane chain in a staggered field and for the quasi-1D ferrimagnetic chain, reflecting the magnetic double structure inherent in these mixed-spin systems.

V. SUMMARY

We have studied the 2D mixed-spin model for which the $s = 1/2$ and $s = 1$ spin chains are stacked alternately. This mixed-spin model includes two interesting spin systems addressed recently: the Haldane gap system in a staggered field as well as the ferrimagnetic chain. By calculating the dispersion relation and the thermodynamic

quantities by means of the Schwinger-boson mean-field theory, we have discussed the magnetic double structure inherent in our mixed-spin systems. In particular, we have treated systematically the quasi-1D Haldane gap system in a staggered magnetic field and also the mixed-spin chain with the ferrimagnetic ground state. This implies that these two spin systems, which have been studied in different contexts experimentally, should possess interesting physics common to the mixed spin systems. We have also found that the results obtained for the staggered-field effect on the Haldane gap system are qualitatively consistent with the experimental findings in the rare-earth compounds $R_2\text{BaNiO}_5$. It remains an interesting problem to evaluate dynamical quantities related to the neutron scattering, etc. Also, it is important to study how the string-order parameter behaves,²³ when the system changes from the Haldane system to the ferrimagnetic chain. These problems are now under consideration.

ACKNOWLEDGMENTS

The work is partly supported by a Grant-in-Aid from the Ministry of Education, Science, Sports, and Culture. A. K. is supported by the Japan Society for the Promotion of Science. N. K. wishes to thank K. Ueda for the warm hospitality at ISSP, University of Tokyo.

¹ F. D. M. Haldane, Phys. Lett. **93A** 464 (1983); F. D. M. Haldane, Phys. Rev. Lett. **50**, 1153 (1983).
² A. Zheludev, E. Ressouche, S. Maslov, T. Yokoo, S. Raymond, and J. Akimitsu, Phys. Rev. Lett. **80**, 3630 (1998).
³ T. Yokoo, A. Zheludev, M. Nakamura, and J. Akimitsu, Phys. Rev. B **55**, 11516 (1997).
⁴ T. Yokoo, S. Raymond, A. Zheludev, S. Maslov, E. Ressouche, I. Zaliznyak, R. Erwin, M. Nakamura, and J. Akimitsu, Phys. Rev. B **58**, 14424 (1998).
⁵ S. Raymond, T. Yokoo, A. Zheludev, S. E. Nagler, A. Wildes, and J. Akimitsu, Phys. Rev. Lett. **82**, 2382 (1999).
⁶ A. Zheludev, S. Maslov, T. Yokoo, J. Akimitsu, S. Raymond, S. E. Nagler, and K. Hirota, cond-matt/9910335
⁷ A. Zheludev, J. M. Tranquada, and T. Vogt, Phys. Rev. B **54**, 6437 (1996).
⁸ J. F. DiTusa *et al.*, Phys. Rev. Lett. **73**, 1857 (1994).
⁹ D. J. Buttrey, J. D. Sullivan, and A. L. Rheingold, J. Solid State Chem. **88**, 291 (1990); E. Garcia-Matres *et al.*, J. Solid State Chem. **103**, 322 (1993); V. Sachan, D. J. Buttrey, J. M. Tranquada, and G. Shirane, Phys. Rev. B **49**, 9658 (1994).
¹⁰ S. Maslov and A. Zheludev, Phys. Rev. B **57** 68 (1998), Phys. Rev. Lett. **80**, 5786 (1998).
¹¹ J. L. Lou, X. Dai, S. Qui, Z. Su, and L. Yu, Phys. Rev. B **60**, 52 (1999).

¹² M. Verdanguer, M. Julve, A. Michalowicz, and O. Kahn, Inorg. Chem. **22**, 2624 (1983).
¹³ G. T. Yee, J. M. Manriquez, D. A. Dixon, R. S. McLean, D. M. Groski, R. B. Flippen, K. S. Narayan, A. J. Epstein, and J. S. Miller, Adv. Mater. **3**, 309 (1991); Inorg. Chem. **22**, 2624 (1983); Inorg. Chem. **26**, 138 (1987).
¹⁴ S. K. Pati, S. Ramasesha, and D. Sen: Phys. Rev. B **55**, 8894 (1997); A. K. Kolezhuk, H.-J. Mikeska, and S. Yamamoto, Phys. Rev. B **55**, R3336 (1997); F. C. Alcaraz and A. L. Malvezzi J. Phys. A **30**, 767 (1997); H. Niggemann, G. Uimin, and J. Zittartz, J. Phys. Cond. Matt. **9**, 9031 (1997).
¹⁵ S. Brehmer, H.-J. Mikeska, and S. Yamamoto, J. Phys. C **9**, 3921 (1997); A. K. Kolezhuk, H.-J. Mikeska, and S. Yamamoto, Phys. Rev. B **55**, R3336 (1997); S. Yamamoto, S. Brehmer, and H.-J. Mikeska, Phys. Rev. B **57**, 13610 (1998).
¹⁶ S. Yamamoto and T. Fukui, Phys. Rev. B **57**, R14008 (1997).
¹⁷ C. Wu, B. Chen, Xi. Dai, Y. Yu, and Z. Su, Phys. Rev. B **60**, 1057 (1999).
¹⁸ D. P. Arovas and A. Auerbach, Phys. Rev. B **38**, 316 (1988); Phys. Rev. Lett. **61**, 617 (1988).
¹⁹ There is another approach based on the modified spin wave theory, which is similar to the SBMFT in many respects. For mixed-spin systems, however, the latter possesses some ambiguity for imposing the constraint to incorporate non-linear effects (see ref. 16), whereas the constraint in the SBMFT is unambiguously introduced by preserving the number of bosons at each site, making the SBMFT more tractable in our case.
²⁰ S. Sarker, C. Jayaprakash, H. R. Krishnamurthy, and M. Ma, Phys. Rev. B **40**, 5028 (1989).
²¹ K. K. Ng, F. C. Zhang, and M. Ma, Phys. Rev. B **53**, 12196 (1996).
²² S. K. Sarker, J. Phys. Condens. Matter **8**, L515 (1996); D. P. Arovas and F. Guinea, Phys. Rev. B **58**, 9150 (1998).
²³ M. den Nijs and K. Rommelse, Phys. Rev. B **40**, 4709 (1989).

Magnetic Double Structure for $S = 1, 1/2$ Mixed-Spin Systems

Yoshihiro Takushima, Akihisa Koga, and Norio Kawakami
Department of Applied Physics, Osaka University, Suita, Osaka 565-0871, Japan
(November 5, 2018)

We investigate the zero-temperature and the finite-temperature properties of the two-dimensional antiferromagnetic quantum spin system composed of the $s = 1/2$ and $s = 1$ spins. The spin excitation spectrum as well as the thermodynamic quantities are computed by means of the Schwinger-boson mean-field theory. We discuss how the magnetic double structure with the gapful and the gapless excitations is generated, and apply the results systematically to the Haldane gap system in a staggered magnetic field and also to the weakly coupled ferrimagnetic mixed-spin chains. It is confirmed that the results obtained are consistent with the experiments for the quasi-one-dimensional Haldane compounds $R_2\text{BaNiO}_5$.

I. INTRODUCTION

The Haldane gap system¹ has been one of the most fascinating subjects in condensed matter physics, for which extensive experimental and theoretical investigations have been providing a variety of new interesting phenomena. One of the hot topics is the magnetic double structure in the quasi-one-dimensional (1D) Haldane systems observed for the rare-earth compounds $R_2\text{BaNiO}_5$.²⁻⁷ In the case with $R = \text{Y}^{3+}$, the system has a disordered ground state with the Haldane gap.⁸ If R is substituted by other magnetic ions such as Nd^{3+} and Pr^{3+} ,^{7,9} the $s = 1/2$ spins on the R^{3+} sublattice order magnetically at low temperatures, thus giving rise to the magnetic double structure composed of the Haldane gap excitation and the gapless excitation induced by the long-range order. This system has been theoretically treated as the Haldane chains with a *static* staggered field which are induced by the ordered $s = 1/2$ spins on the R^{3+} sublattice so far.^{10,11} In a recent paper,⁵ however, it has been pointed out that the dynamics of the $s = 1/2$ spins may be also important, stimulating us to treat the system by a mixed-spin model. Concerning the magnetic double structure, there is another interesting spin system of current interest, i.e. the quantum ferrimagnetic chain composed of two kinds of mixed spins.¹²⁻¹⁷ Several compounds have been already found, which indeed realize the mixed-spin system.^{12,13} This has been stimulating further intensive theoretical studies on this subject.¹⁴⁻¹⁷ In particular, it has been pointed out that such a ferrimagnetic chain has the double structure for the spin excitation spectrum, which controls the characteristic properties in the ferrimagnetic chain.¹⁶

The above two subjects, which have been studied experimentally in different contexts, should possess the common interesting physics, because both systems are

characterized by the mixture of two kinds of distinct spins. Motivated by these hot topics, we here study the properties of the antiferromagnetic mixed-spin system in detail, for which the $s = 1$ and $s = 1/2$ spin chains are stacked alternately. We exploit the two-dimensional (2D) system as the simplest model which possesses the magnetic long-range order at zero temperature. By computing the dispersion relation and the staggered magnetization by means of the Schwinger-boson mean-field theory,¹⁸ we clarify how our system generates the magnetic double structure, which naturally interpolates the above two interesting spin systems. We also show that the results obtained are consistent with the experimental findings for quasi-1D Haldane compounds $R_2\text{BaNiO}_5$.²⁻⁷

This paper is organized as follows. We introduce the model and then briefly summarize the Schwinger-boson techniques in Sec. II. We discuss the zero-temperature properties in Sec. III, and finally move to the thermodynamic properties in Sec. IV. A brief summary is given in Sec. V.

II. SCHWINGER-BOSON MEAN-FIELD THEORY

Let us consider a 2D mixed-spin model on the square lattice, which is described by the following Hamiltonian,

$$H = J_1 \sum_{i,j,\eta} \left[\mathbf{S}_{2i,2j}^{A_1} \cdot \mathbf{S}_{2i+\eta,2j}^{B_1} + \mathbf{S}_{2i+\eta,2j+1}^{B_2} \cdot \mathbf{S}_{2i,2j+1}^{A_2} \right] \\ + \sum_{i,j,\eta} \left[J_2 \mathbf{S}_{2i,2j}^{A_1} \cdot \mathbf{S}_{2i,2j+\eta}^{A_2} + J_3 \mathbf{S}_{2i+1,2j}^{B_1} \cdot \mathbf{S}_{2i+1,2j+\eta}^{B_2} \right], \quad (1)$$

where $\mathbf{S}_{i,j}^A$ ($\mathbf{S}_{i,j}^B$) is the spin operator at the (i,j) -th site in the (x,y) plane, and η implies the summation to be taken over nearest-neighbor sites. All the exchange couplings J_1 , J_2 and J_3 are assumed to be antiferromagnetic. We here focus on the mixed-spin system composed of $S^A = 1/2$ and $S^B = 1$ spins, since it is straightforward to generalize the results to the arbitrary-spin case. In Fig. 1, we have drawn the mixed-spin model schematically. The indices A_m and B_m label the sublattice in the unit cell. Note that this mixed-spin model is constructed in two ways depending on how we stack the independent spin chains by introducing three kinds of the coupling constants. By taking $J_3 \gg J_1, J_2$, we can study the characteristic properties of the $s = 1$ Haldane spin chains coupled with the $s = 1/2$ gapless spin chains, which may have the relevance to the Haldane gap system in a staggered field observed in the compounds $R_2\text{BaNiO}_5$.²⁻⁷ On the other hand, by setting the coupling constants

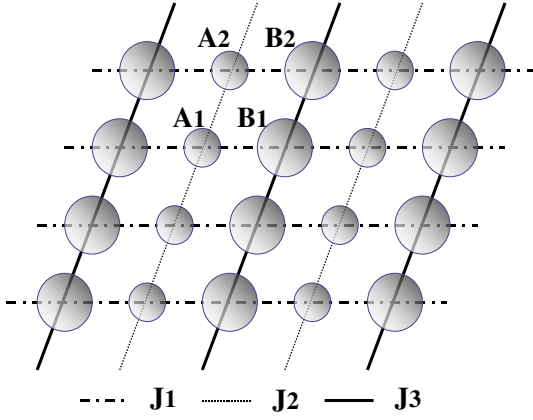


FIG. 1. 2D mixed-spin model on a square lattice. The small (large) circle represents $S^A = 1/2$ ($S^B = 1$) spin. The bold dashed, the thin dashed and the bold solid lines represent the coupling constants J_1 , J_2 and J_3 , respectively. A_1, A_2, B_1 and B_2 specify four spins in the unit cell.

$J_1 \gg J_2, J_3$, we can investigate how the independent ferromagnetic chains ($J_2 = J_3 = 0$), which have been studied extensively in recent years,^{12–17} are combined to form the 2D system. The advantage of our mixed-spin approach is that we can systematically describe these two interesting systems by continuously varying the parameters J_1 , J_2 and J_3 .

We employ the Schwinger-boson mean-field theory (SBMFT)¹⁸ to study the above mixed-spin model.¹⁹ This method was applied successfully to the 2D Heisenberg model with uniform spins,^{18,20} and then to the bilayer system,²¹ the double-exchange system,²² the ferrimagnetic chain,¹⁷ etc. It is known that the SBMFT can describe the magnetically ordered phase, which is characterized by the condensation of the Schwinger-bosons.²⁰ In the Schwinger-boson representation, the spin operators are expressed in terms of the boson creation and annihilation operators $\gamma_\alpha^\dagger, \gamma_\alpha$, with the Pauli matrix σ as $\mathbf{S} = \frac{1}{2}\gamma_\alpha^\dagger \sigma_{\alpha\beta} \gamma_\beta$ ($\alpha, \beta = \uparrow, \downarrow$). Since the unit cell in our model includes four sites, we necessarily introduce eight kinds of Bose operators $\gamma_\alpha = a_\alpha^{(1)}, a_\alpha^{(2)}, b_\alpha^{(1)}, b_\alpha^{(2)}$ which belong to the A_1, A_2, B_1, B_2 sublattices, respectively. By imposing the constraint $\gamma_{i\uparrow}^\dagger \gamma_{i\uparrow} + \gamma_{i\downarrow}^\dagger \gamma_{i\downarrow} = 2S^A$ or $2S^B$ on each site, we can correctly map the original spin system to the boson system. Introducing the Lagrange multipliers λ_{ij}^A and λ_{ij}^B , the Hamiltonian with the constraints is recast to

$$\begin{aligned}
H = & -2 \sum_{i,j,\eta} \left[J_1 \left(A_{ij\eta}^\dagger A_{ij\eta} + B_{ij\eta}^\dagger B_{ij\eta} \right) \right. \\
& + J_2 C_{ij\eta}^\dagger C_{ij\eta} + J_3 D_{ij\eta}^\dagger D_{ij\eta} \left. \right] \\
& + \sum_{n=1}^2 \left[\sum_{(ij) \in A_n} \lambda_{ij}^A \left(\sum_{\sigma} a_{ij\sigma}^{(n)\dagger} a_{ij\sigma}^{(n)} - 2S^A \right) \right.
\end{aligned}$$

$$\begin{aligned}
& + \sum_{(ij) \in B_n} \lambda_{ij}^B \left(\sum_{\sigma} b_{ij\sigma}^{(n)\dagger} b_{ij\sigma}^{(n)} - 2S^B \right) \left. \right] \\
& + \sum_{i,j,\eta} \left[J_1 (S^{A_1} S^{B_1} + S^{A_2} S^{B_2}) \right. \\
& + J_2 S^{A_1} S^{A_2} + J_3 S^{B_1} S^{B_2} \left. \right], \quad (2)
\end{aligned}$$

where four bond operators are introduced as

$$A_{ij\eta} = a_{2i,2j\uparrow}^{(1)} b_{2i+\eta,2j\downarrow}^{(1)} - a_{2i,2j\downarrow}^{(1)} b_{2i+\eta,2j\uparrow}^{(1)}, \quad (3)$$

$$B_{ij\eta} = a_{2i,2j+1\uparrow}^{(2)} b_{2i+\eta,2j+1\downarrow}^{(2)} - a_{2i,2j+1\downarrow}^{(2)} b_{2i+\eta,2j+1\uparrow}^{(2)}, \quad (4)$$

$$C_{ij\eta} = a_{2i,2j\uparrow}^{(1)} a_{2i,2j+\eta\downarrow}^{(2)} - a_{2i,2j\downarrow}^{(1)} a_{2i,2j+\eta\uparrow}^{(2)}, \quad (5)$$

$$D_{ij\eta} = b_{2i+1,2j\uparrow}^{(1)} b_{2i+1,2j+\eta\downarrow}^{(2)} - b_{2i+1,2j\downarrow}^{(1)} b_{2i+1,2j+\eta\uparrow}^{(2)}. \quad (6)$$

We perform a Hartree-Fock decomposition of eq. (2) by taking the thermal average $\langle A_{ij\eta} \rangle = A$, $\langle \lambda_{ij}^A \rangle = \lambda_A$, etc., which means that these values are assumed to be uniform and static.

By diagonalizing the mean-field Hamiltonian via the Bogoliubov transformation, we have

$$H_{\text{MF}} = \sum_{\mathbf{k}\sigma} \sum_{n=1}^2 \left[E_{\mathbf{k}}^{(1)} \alpha_{\mathbf{k}\sigma}^{(n)\dagger} \alpha_{\mathbf{k}\sigma}^{(n)} + E_{\mathbf{k}}^{(2)} \beta_{\mathbf{k}\sigma}^{(n)\dagger} \beta_{\mathbf{k}\sigma}^{(n)} \right], \quad (7)$$

where α and β are the Bose operators for normal modes. The corresponding energy spectrums read

$$E_{\mathbf{k}}^{(1)} = \sqrt{\frac{E_0 - \sqrt{E_1}}{2}}, \quad E_{\mathbf{k}}^{(2)} = \sqrt{\frac{E_0 + \sqrt{E_1}}{2}}, \quad (8)$$

where E_0 and E_1 are given by

$$E_0 = \lambda_A^2 + \lambda_B^2 - 2d_{\mathbf{k}}^2 - e_{\mathbf{k}}^2 - f_{\mathbf{k}}^2, \quad (9)$$

$$E_1 = (\lambda_A^2 - \lambda_B^2 - e_{\mathbf{k}}^2 + f_{\mathbf{k}}^2)^2$$

$$-4d_{\mathbf{k}}^2 \left((\lambda_A - \lambda_B)^2 - (e_{\mathbf{k}} + f_{\mathbf{k}})^2 \right),$$

with

$$d_{\mathbf{k}} = 2AJ_1 \cos k_x, \quad e_{\mathbf{k}} = 2CJ_2 \cos k_y, \\ f_{\mathbf{k}} = 2DJ_3 \cos k_y.$$

By minimizing the free energy thus obtained at finite temperatures, we end up with the self-consistent equations for $A = B, C, D, \lambda_A, \lambda_B$,

$$1 + 2S^A = \sum_n \int \frac{d\mathbf{k}}{\pi^2} \coth \kappa E_{\mathbf{k}}^{(n)} \frac{\partial E_{\mathbf{k}}^{(n)}}{\partial \lambda_A}, \quad (10)$$

$$1 + 2S^B = \sum_n \int \frac{d\mathbf{k}}{\pi^2} \coth \kappa E_{\mathbf{k}}^{(n)} \frac{\partial E_{\mathbf{k}}^{(n)}}{\partial \lambda_B}, \quad (11)$$

$$-8J_1 A = \sum_n \int \frac{d\mathbf{k}}{\pi^2} \coth \kappa E_{\mathbf{k}}^{(n)} \frac{\partial E_{\mathbf{k}}^{(n)}}{\partial A}, \quad (12)$$

$$-4J_2C = \sum_n \int \frac{d\mathbf{k}}{\pi^2} \coth \kappa E_{\mathbf{k}}^{(n)} \frac{\partial E_{\mathbf{k}}^{(n)}}{\partial C}, \quad (13)$$

$$-4J_3D = \sum_n \int \frac{d\mathbf{k}}{\pi^2} \coth \kappa E_{\mathbf{k}}^{(n)} \frac{\partial E_{\mathbf{k}}^{(n)}}{\partial D}, \quad (14)$$

with $\kappa = 1/(2k_B T)$, where we have assumed that the bond operators which link the $s = 1$ and $s = 1/2$ spins take the same mean value, $A = B$. This completes our formulation based on the SBMFT. In the following sections, we solve these self-consistent equations to estimate the excitation spectrum and the thermodynamic quantities. Since it is not easy to analytically perform the Bogoliubov transformation, we numerically diagonalize the mean-field Hamiltonian to compute the energy dispersions $E_{\mathbf{k}}^{(1)}$ and $E_{\mathbf{k}}^{(2)}$.

III. PROPERTIES AT ZERO TEMPERATURE

In order to treat the ground state properties, it should be taken into account that the Bogoliubov particles of the α branch in eq.(7) may condense at absolute zero, because the excitation energy $E_{\mathbf{k}}^{(1)}$ has its minimal value $E_{\mathbf{k}}^{(1)} = 0$ at $\mathbf{k} = \mathbf{0}$ while the β branch has a finite gap even at $T = 0$. Sarker *et al.*²⁰ showed that the long-range order is described by the condensation of the Schwinger-bosons for the ferromagnetic and antiferromagnetic Heisenberg models. This is also the case for our 2D mixed-spin model on a square lattice.

Suppose that the bosons condense at the states of $\alpha_{\uparrow}^{(1)}|_{\mathbf{k}=\mathbf{0}}$ and $\alpha_{\downarrow}^{(2)}|_{\mathbf{k}=\mathbf{0}}$, by fictitiously applying an infinitesimal external staggered field to the A and B lattices. The self-consistent equations at $T = 0$, which include the Bose condensation, now read,

$$\Gamma = \frac{2}{N^2} \coth \kappa E_{\mathbf{k}=\mathbf{0}}^{(1)} \Big|_{\kappa \rightarrow \infty} = \frac{\left[1 + 2S^A - \sum_n \int \frac{d\mathbf{k}}{\pi^2} \frac{\partial E_{\mathbf{k}}^{(n)}}{\partial \lambda_A} \right]}{\partial E_{\mathbf{k}=\mathbf{0}}^{(1)} / \partial \lambda_A}, \quad (15)$$

$$1 + 2S^B = \Gamma \frac{\partial E_{\mathbf{k}}^{(1)}}{\partial \lambda_B} \Big|_{\mathbf{k}=\mathbf{0}} + \sum_n \int \frac{d\mathbf{k}}{\pi^2} \frac{\partial E_{\mathbf{k}}^{(n)}}{\partial \lambda_B}, \quad (16)$$

$$-4A = \Gamma \frac{\partial E_{\mathbf{k}}^{(1)}}{\partial d_{\mathbf{k}}} \Big|_{\mathbf{k}=\mathbf{0}} + \sum_n \int \frac{d\mathbf{k}}{\pi^2} \cos k_x \frac{\partial E_{\mathbf{k}}^{(n)}}{\partial d_{\mathbf{k}}}, \quad (17)$$

$$-2C = \Gamma \frac{\partial E_{\mathbf{k}}^{(1)}}{\partial e_{\mathbf{k}}} \Big|_{\mathbf{k}=\mathbf{0}} + \sum_n \int \frac{d\mathbf{k}}{\pi^2} \cos k_y \frac{\partial E_{\mathbf{k}}^{(n)}}{\partial e_{\mathbf{k}}}, \quad (18)$$

$$-2D = \Gamma \frac{\partial E_{\mathbf{k}}^{(1)}}{\partial f_{\mathbf{k}}} \Big|_{\mathbf{k}=\mathbf{0}} + \sum_n \int \frac{d\mathbf{k}}{\pi^2} \cos k_y \frac{\partial E_{\mathbf{k}}^{(n)}}{\partial f_{\mathbf{k}}}. \quad (19)$$

We shall solve these equations numerically for given coupling constants J_1, J_2 and J_3 .

A. Dispersion relation

We start our discussions with the case that may be regarded as the Haldane gap system in a staggered field. When $J_1 = 0$, the 2D system is completely decoupled into the $s = 1$ massive Haldane chains and the $s = 1/2$ massless spin chains. When we introduce the interchain couplings among them, the ground state has the long-range order mainly due to the $s = 1/2$ spins. The important point is that even though we have the long-range order, the Haldane-type gapful excitation still exists. Therefore, as far as the case with small J_1 and J_2 is concerned, the system is regarded as the one often called the Haldane gap system in a staggered field.²⁻⁷ In Fig. 2, we show the dispersion relation calculated for $J_1 = J_2 = 1/2$ and $J_3 = 1$. As seen in this figure, the lower branch

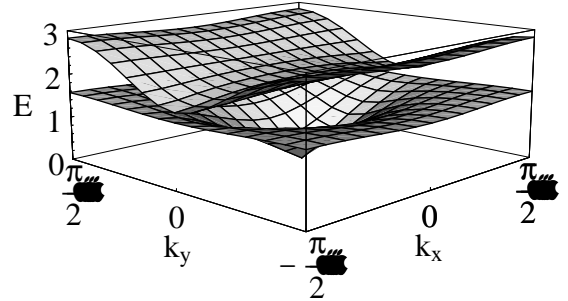


FIG. 2. The excitation spectrum for the mixed-spin model which may be regarded as the *Haldane gap in a staggered field* ($J_1 = J_2 = 1/2, J_3 = 1$). Note that the Brillouin zone is reduced to a quarter of that for the uniform spin case, since the unit cell now includes the four sites.

is gapless with linear dispersion relation, reflecting the antiferromagnetic long-range order, whereas the upper optical mode is mainly composed of the Haldane-type excitation. It is observed that the dispersion in the k_x -direction is indeed weak for the optical mode, since the interchain coupling is much smaller than the energy gap for the optical mode, which confirms that the system in Fig. 2 may be regarded as the Haldane gap system in a staggered field. Although we have also performed the calculation for the cases with smaller J_1 and J_2 , the obtained dispersion of the optical branch becomes almost flat in the k_x -direction, so that we have not shown them here. Concerning this limit of small J_1 , we here make a brief comment on the validity of the SBMFT. When J_1 takes too small value, for which the system is almost decoupled into independent $s = 1$ and $s = 1/2$ chains, the SBMFT may lead to a pathological result: although the Haldane gap for the $s = 1$ chain is well described by the SBMFT, it is not the case for the gapless $s = 1/2$ chains, for which we are left with a gapful phase. Actually, if the value of J_1 ($= J_2$) becomes smaller than $J_1/J_3 \sim 10^{-2}$,

we encounter a problem that the present self-consistent calculation does not converge, implying that our assumption for the antiferromagnetic ordered state does not hold anymore. Nevertheless, we find that the correct behavior with the antiferromagnetic ground state is still obtained except for this small parameter region.

By increasing the coupling parameters J_2, J_3 continuously, we naturally enter in the 2D ordered mixed-spin system. Note that although during this process the magnetic double structure is kept unchanged in its typical feature, the nature of the optical mode is gradually changed from the Haldane-gap excitation: i.e. the gapful excitation may be equally contributed from both the $s = 1$ and $s = 1/2$ spin sectors. As a reference, we show the dispersion relation for the mixed-spin model with the isotropic bonds $J_1 = J_2 = J_3 = 1$ in Fig. 3. If we further decrease

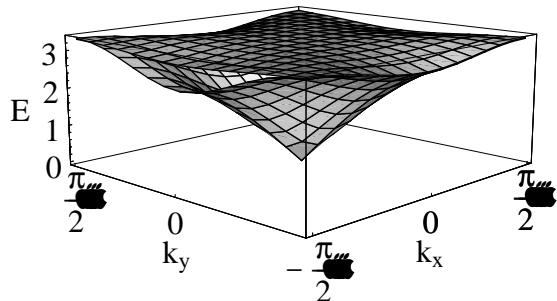


FIG. 3. The excitation spectrum for the 2D mixed-spin model ($J_1 = J_2 = J_3 = 1$).

the couplings J_2 and J_3 , the system gradually approaches the quasi-1D ferrimagnetic chains with the periodic arrangement of spins $1/2 \circ 1 \circ 1/2 \circ 1$. The dispersion relation obtained in the corresponding parameter region is shown in Fig. 4. Now the optical mode with a weak disper-

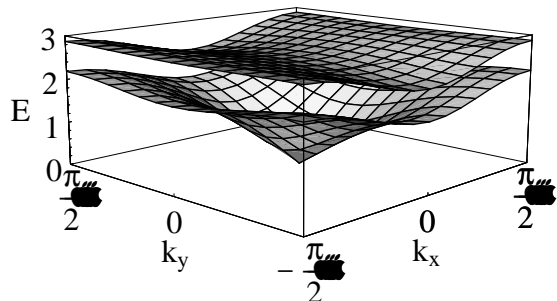


FIG. 4. The excitation spectrum for the *coupled ferrimagnetic chains* ($J_1 = 1, J_2 = J_3 = 1/2$).

sion in the k_y -direction is essentially the same as that found for the ferrimagnetic chain.¹⁶ In order to clearly observe how the gapless dispersion changes its character in the ferrimagnetic-chain limit, we have shown the low-energy dispersion relation at $k_y=0$ in Fig. 5. It is seen that with the decrease of the coupling constants J_2 and J_3 , the k_x -linear dependence is gradually changed to the k_x^2 dependence characteristic of the ferrimagnetic chain except for the small k_x region where the 2D an-

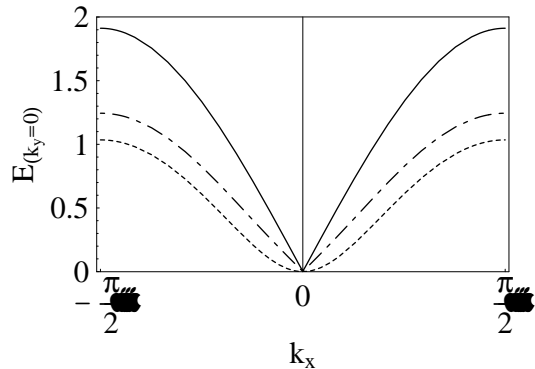


FIG. 5. The gapless dispersion for the *coupled ferrimagnetic chains* at $k_y=0$. The solid, the dash-dotted and the dashed lines correspond to the cases of $J_2 = J_3 = 0.5, 0.1$ and 0 ($J_1 = 1$).

tiferromagnetic order still gives rise to the k_x -linear dependence. At $J_2 = J_3 = 0$, the system is reduced to the isolated ferrimagnetic chains, for which the 2D character completely disappears, and thus the gapless dispersion simply follows the k_x^2 dependence. We note that the ferrimagnetic chains have been experimentally realized in the compounds such as $\text{NiCu}(\text{C}_2\text{O}_4)_2 \cdot 4\text{H}_2\text{O}$ and $\text{MnCu}(\text{pba})(\text{H}_2\text{O})_3 \cdot 2\text{H}_2\text{O}$,¹³ and have been studied theoretically by many groups.^{14–16} Among others, it has been reported¹⁶ that this system exhibits the dual properties consistent with our results: the physical quantities are controlled by the $s = 1$ antiferromagnetic spin chain at high temperatures and by the effective $s = 1/2$ ferromagnetic spin chain at low temperatures.

The above analysis of the excitation spectrum implies that the quasi-1D Haldane gap system in a staggered field^{2–7} and the quasi-1D weakly coupled ferrimagnetic chains,^{12,13} which have been studied in different contexts experimentally, share common interesting physics inherent in the mixed-spin systems. In particular, it is highly desirable to experimentally observe the magnetic double structure in the excitation spectrum for the ferrimagnetic-chain compounds.

B. Haldane gap in a staggered field

Let us discuss the case of the Haldane gap system in a staggered field in more detail. We here observe how the effective staggered field induced by the $s = 1/2$ spin chains affects the properties of the Haldane gap, by changing the coupling constants J_1 and J_2 . For small values of J_1 and J_2 , we define the effective staggered field on the $s = 1$ Haldane chain by $H_{\text{ST}}^{\text{eff}} = J_1 \langle S_z^A \rangle$, where $\langle S_z^A \rangle$ is the spontaneous staggered magnetization of the $s = 1/2$ spin chain. We numerically estimate the effective staggered field, and show the obtained results in Fig. 6. It is seen that the effective staggered field increases monotonously with the increase of J_1 and J_2 , as should be expected. In a similar way, we also compute

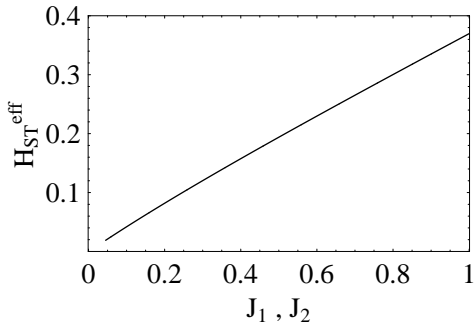


FIG. 6. The effective staggered field $H_{\text{ST}}^{\text{eff}}$ as a function of the coupling constant J_1 ($=J_2$) where we set $J_3 = 1$.

the staggered magnetization $\langle S_z^B \rangle$ of the $s = 1$ spin chains, and as well as the Haldane gap which is defined as the minimum of the excitation energy in the optical branch $\Delta = E_{\mathbf{k}=(\frac{\pi}{2},0)}^{(2)}$. These quantities are shown in

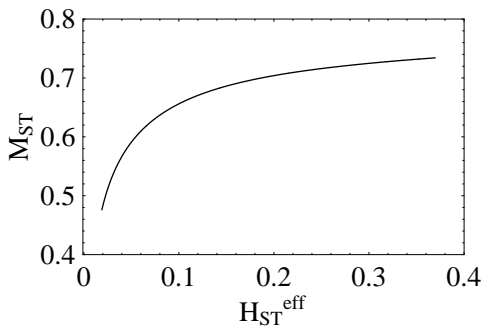


FIG. 7. Plots of the staggered magnetization M_{ST} as a function of the effective staggered magnetic field.

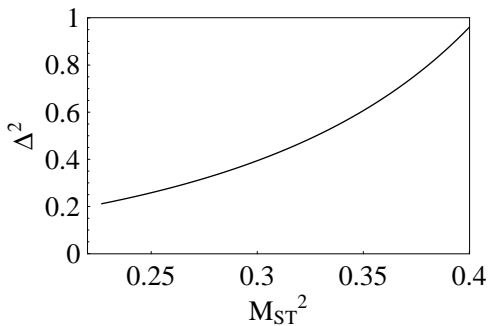


FIG. 8. Plots of the square of the Haldane gap Δ as a function of the square of the staggered magnetization M_{ST} .

Figs. 7 and 8. Following the way used for the experimental analysis,^{2,4} we have plotted the staggered magnetization (the square of the Haldane gap) as a function of the effective staggered field (the square of the staggered magnetization). It is seen that as the staggered field is increased, the staggered magnetization as well as the Haldane gap Δ are increased, being consistent with the result pointed out for the Haldane chain system with a *static* magnetic field.^{10,11}

Since we are dealing with the 2D model at zero temperature, our results may not be directly applied to the experiments. Nevertheless, we can confirm whether the present results are consistent with the experiments for the rare-earth compounds $R_2\text{BaNiO}_5$ ²⁻⁷ with $R = \text{Nd}^{3+}$ or Pr^{3+} .^{7,9} Experimentally, as the temperature is decreased, the system shows the phase transition to the magnetically ordered phase. When the temperature is further decreased, the staggered moment for the $s = 1/2$ sector develops, and thereby gives rise to the increase of the staggered field, which indeed enhances the magnitude of the Haldane gap.^{10,11} Also, the staggered moment on the Haldane chains increases, as should be expected. These characteristic features are consistent with our results, and in particular, the qualitative behaviors for the staggered magnetization and the Haldane gap shown in Figs. 7 and 8 agree fairly well with experimental findings.^{2,4}

C. Coupled ferrimagnetic chains

Before closing this section, we briefly discuss the case close to the ferrimagnetic chain, which is realized by taking the limit of $J_1 \gg J_2, J_3$. Even in this one-dimensional limit, the system still exhibits the antiferromagnetic order as far as J_2 and J_3 take finite values. As mentioned above, at $J_2 = J_3 = 0$, the system shows the ferrimagnetic order, and hence the dispersion relation for the acoustic mode is changed to the quadratic one.¹⁵⁻¹⁷ In this way, the crossover-like behavior is seen in the gapless mode, whereas much simpler behavior is observed in the gapful mode. In Fig. 9, we display the spin gap Δ for the optical branch in the ferrimagnetic-chain limit. With decreasing J_2 and J_3 , the spin gap monotonically decreases, and reaches the value of $\Delta=1.778$ at $J_2 = J_3 = 0$, which is very close to that of the quantum Monte Carlo method, $\Delta=1.767$,¹⁵ as already demonstrated by Wu *et al.*¹⁷ In this way, in the ferrimagnetic-chain limit, the SBMFT may provide the reliable estimates of the physical quantities even at quantitative level. As discussed by Yamamoto and Fukui,¹⁶ this optical mode is mainly composed of excitations in the effective $s = 1$ antiferromagnetic spin chain, whereas the acoustic mode is given by excitations in the effective $s = 1/2$ ferromagnetic chain.

IV. THERMODYNAMIC PROPERTIES AT FINITE TEMPERATURES

We now move to the thermodynamic properties at finite temperatures. The self-consistent equations (10)-(14) are solved numerically at finite temperatures to obtain the thermodynamic quantities. We here briefly summarize the results obtained. In the previous section, it has been shown that even for the set of the parameters $J_1 = J_2 = 1/2, J_3 = 1$ ($J_1 = 1, J_2 = J_3 = 1/2$), the

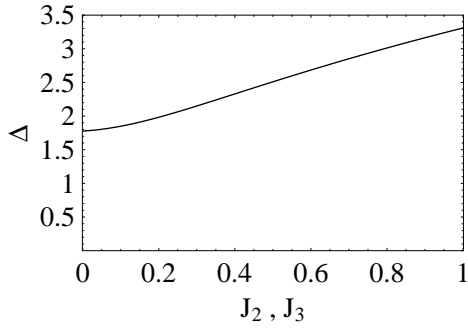


FIG. 9. Plots of the spin gap for the optical branch in the limit of the coupled ferrimagnetic chains ($J_2 = J_3$).

system may be approximately described by the Haldane gap system in a staggered field (coupled ferrimagnetic chains), so that we shall show the results for these parameters below. We start with the effective spin gaps

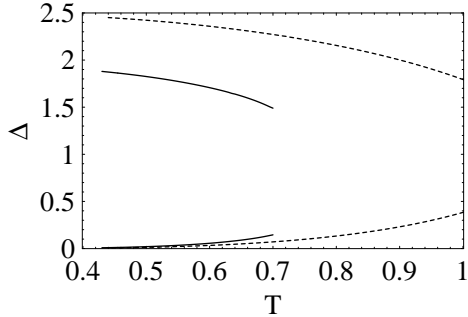


FIG. 10. The spin gaps for the optical and acoustic branches as a function of the temperature T : the solid lines correspond to the case for $J_1 = J_2 = 1/2, J_3 = 1$ while the dashed lines for $J_1 = 1, J_2 = J_3 = 1/2$. Note that at higher temperatures our SBMF approach breaks down, so that we have plotted the data available for each choice of parameters.

calculated at finite temperatures, which are shown as a function of the temperature in Fig. 10. It is seen that both of the two cases exhibit similar temperature dependence in the spin gap. For each case, there are two distinct spin gaps, corresponding respectively to the optical mode and the acoustic mode, reflecting the double structure for the excitation spectrum. Note that both of two modes should be massive at finite temperatures. It may be physically sensible to regard these spin gaps as the inverse of the correlation lengths. As should be expected, the spin gap for the optical mode increases up to the zero-temperature value with the decrease of the temperature. On the other hand, the spin gap for the acoustic mode decreases, leading to the divergent correlation length which characterizes the magnetically ordered state at $T = 0$.

The uniform and staggered spin susceptibilities, χ_{uni} and χ_{stag} , are calculated by using the standard linear-response formulae,

$$\chi_{\text{uni}} = \sum_{i,j=1,2} [\langle \langle S_z^{A_i} S_z^{A_j} \rangle \rangle_{\mathbf{q},\omega} + \langle \langle S_z^{B_i} S_z^{B_j} \rangle \rangle_{\mathbf{q},\omega} + 2\langle \langle S_z^{A_i} S_z^{B_j} \rangle \rangle_{\mathbf{q},\omega}] |_{\mathbf{q},\omega \rightarrow 0}, \quad (20)$$

$$\chi_{\text{stag}} = \sum_{i,j=1,2} [(-1)^{i+j} (\langle \langle S_z^{A_i} S_z^{A_j} \rangle \rangle_{\mathbf{q},\omega} + \langle \langle S_z^{B_i} S_z^{B_j} \rangle \rangle_{\mathbf{q},\omega}) + 2(-1)^{i+j+1} \langle \langle S_z^{A_i} S_z^{B_j} \rangle \rangle_{\mathbf{q},\omega}] |_{\mathbf{q},\omega \rightarrow 0}, \quad (21)$$

where $\langle \langle S_z^{A_i} S_z^{A_j} \rangle \rangle_{\mathbf{q},\omega}$, etc., are the retarded spin correlation functions. In Fig. 11, we plot the effective Curie

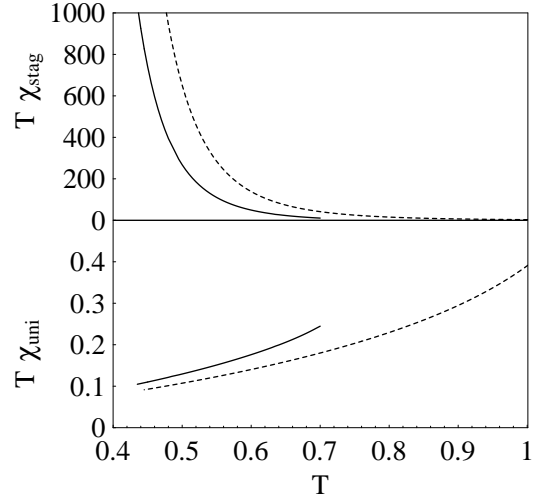


FIG. 11. Plots of $T\chi_{\text{stag}}$ for the staggered susceptibility and $T\chi_{\text{uni}}$ for the uniform susceptibility as a function of the temperature T : the solid lines for $J_1 = J_2 = 1/2, J_3 = 1$ and the dashed lines for $J_1 = 1, J_2 = J_3 = 1/2$

constants $T\chi_{\text{uni}}$ and $T\chi_{\text{stag}}$ as a function of T . It is seen that the effective Curie constant for the uniform sector is gradually decreased as the temperature is decreased, while that for the staggered sector diverges, implying that the antiferromagnetic correlation is enhanced at low temperatures.

As seen from the above results, the thermodynamic properties at finite temperatures show quite similar behavior both for the Haldane chain in a staggered field and for the quasi-1D ferrimagnetic chain, reflecting the magnetic double structure inherent in these mixed-spin systems.

V. SUMMARY

We have studied the 2D mixed-spin model for which the $s = 1/2$ and $s = 1$ spin chains are stacked alternately. This mixed-spin model includes two interesting spin systems addressed recently: the Haldane gap system in a staggered field as well as the ferrimagnetic chain. By calculating the dispersion relation and the thermodynamic

quantities by means of the Schwinger-boson mean-field theory, we have discussed the magnetic double structure inherent in our mixed-spin systems. In particular, we have treated systematically the quasi-1D Haldane gap system in a staggered magnetic field and also the mixed-spin chain with the ferrimagnetic ground state. This implies that these two spin systems, which have been studied in different contexts experimentally, should possess interesting physics common to the mixed spin systems. We have also found that the results obtained for the staggered-field effect on the Haldane gap system are qualitatively consistent with the experimental findings in the rare-earth compounds $R_2\text{BaNiO}_5$. It remains an interesting problem to evaluate dynamical quantities related to the neutron scattering, etc. Also, it is important to study how the string-order parameter behaves,²³ when the system changes from the Haldane system to the ferrimagnetic chain. These problems are now under consideration.

ACKNOWLEDGMENTS

The work is partly supported by a Grant-in-Aid from the Ministry of Education, Science, Sports, and Culture. A. K. is supported by the Japan Society for the Promotion of Science. N. K. wishes to thank K. Ueda for the warm hospitality at ISSP, University of Tokyo.

-
- ¹ F. D. M. Haldane, Phys. Lett. **93A** 464 (1983); F. D. M. Haldane, Phys. Rev. Lett. **50**, 1153 (1983).
² A. Zheludev, E. Ressouche, S. Maslov, T. Yokoo, S. Raymond, and J. Akimitsu, Phys. Rev. Lett. **80**, 3630 (1998).
³ T. Yokoo, A. Zheludev, M. Nakamura, and J. Akimitsu, Phys. Rev. B **55**, 11516 (1997).
⁴ T. Yokoo, S. Raymond, A. Zheludev, S. Maslov, E. Ressouche, I. Zaliznyak, R. Erwin, M. Nakamura, and J. Akimitsu, Phys. Rev. B **58**, 14424 (1998).
⁵ S. Raymond, T. Yokoo, A. Zheludev, S. E. Nagler, A. Wildes, and J. Akimitsu, Phys. Rev. Lett. **82**, 2382 (1999).
⁶ A. Zheludev, S. Maslov, T. Yokoo, J. Akimitsu, S. Raymond, S. E. Nagler, and K. Hirota, cond-matt/9910335
⁷ A. Zheludev, J. M. Tranquada, and T. Vogt, Phys. Rev. B **54**, 6437 (1996).
⁸ J. F. DiTusa *et al.*, Phys. Rev. Lett. **73**, 1857 (1994).
⁹ D. J. Buttrey, J. D. Sullivan, and A. L. Rheingold, J. Solid State Chem. **88**, 291 (1990); E. Garcia-Matres *et al.*, J. Solid State Chem. **103**, 322 (1993); V. Sachan, D. J. Buttrey, J. M. Tranquada, and G. Shirane, Phys. Rev. B **49**, 9658 (1994).
¹⁰ S. Maslov and A. Zheludev, Phys. Rev. B **57** 68 (1998), Phys. Rev. Lett. **80**, 5786 (1998).
¹¹ J. L. Lou, X. Dai, S. Qui, Z. Su, and L. Yu, Phys. Rev. B **60**, 52 (1999).

- ¹² M. Verdanguer, M. Julve, A. Michalowicz, and O. Kahn, Inorg. Chem. **22**, 2624 (1983).
¹³ G. T. Yee, J. M. Manriquez, D. A. Dixon, R. S. McLean, D. M. Groski, R. B. Flippen, K. S. Narayan, A. J. Epstein, and J. S. Miller, Adv. Mater. **3**, 309 (1991); Inorg. Chem. **22**, 2624 (1983); Inorg. Chem. **26**, 138 (1987).
¹⁴ S. K. Pati, S. Ramasesha, and D. Sen: Phys. Rev. B **55**, 8894 (1997); A. K. Kolezhuk, H.-J. Mikeska, and S. Yamamoto, Phys. Rev. B **55**, R3336 (1997); F. C. Alcaraz and A. L. Malvezzi J. Phys. A **30**, 767 (1997); H. Niggemann, G. Uimin, and J. Zittartz, J. Phys. Cond. Matt. **9**, 9031 (1997).
¹⁵ S. Brehmer, H.-J. Mikeska, and S. Yamamoto, J. Phys. C **9**, 3921 (1997); A. K. Kolezhuk, H.-J. Mikeska, and S. Yamamoto, Phys. Rev. B **55**, R3336 (1997); S. Yamamoto, S. Brehmer, and H.-J. Mikeska, Phys. Rev. B **57**, 13610 (1998).
¹⁶ S. Yamamoto and T. Fukui, Phys. Rev. B **57**, R14008 (1997).
¹⁷ C. Wu, B. Chen, Xi. Dai, Y. Yu, and Z. Su, Phys. Rev. B **60**, 1057 (1999).
¹⁸ D. P. Arovas and A. Auerbach, Phys. Rev. B **38**, 316 (1988); Phys. Rev. Lett. **61**, 617 (1988).
¹⁹ There is another approach based on the modified spin wave theory, which is similar to the SBMFT in many respects. For mixed-spin systems, however, the latter possesses some ambiguity for imposing the constraint to incorporate non-linear effects (see ref. 16), whereas the constraint in the SBMFT is unambiguously introduced by preserving the number of bosons at each site, making the SBMFT more tractable in our case.
²⁰ S. Sarker, C. Jayaprakash, H. R. Krishnamurthy, and M. Ma, Phys. Rev. B **40**, 5028 (1989).
²¹ K. K. Ng, F. C. Zhang, and M. Ma, Phys. Rev. B **53**, 12196 (1996).
²² S. K. Sarker, J. Phys. Condens. Matter **8**, L515 (1996); D. P. Arovas and F. Guinea, Phys. Rev. B **58**, 9150 (1998).
²³ M. den Nijs and K. Rommelse, Phys. Rev. B **40**, 4709 (1989).